Different Modes of Reactivity of Cp*W(NO)(alkyl)(η^3-allyl) Complexes with Cyclic Amines: The Influence of the Allyl Ligands

Jenkins Y. K. Tsang, Miriam S. A. Buschhaus, Chikako Fujita-Takayama, Brian O. Patrick, and Peter Legzdins*

Department of Chemistry, The University of British Columbia, Vancouver, British Columbia, Canada V6T 1Z1

Received December 10, 2007

Metathesis reactions between Cp*W(NO)(CH_2EMe_3)Cl (E = C or Si) and a variety of bis(allyl)magnesium reagents lead to the formation of 18e Cp*W(NO)(alkyl)(η^3-allyl) complexes. The compounds Cp*W(NO)(CH_2CMe_3)(η^3-CH_2CHCMe_2) (**1**), Cp*W(NO)(CH_2CMe_3)(η^3-CH_2CMeCH_2) (**2**), Cp*W(NO)(CH_2CMe_3)(η^3-$CH_2CHCHMe$) (**3**), Cp*W(NO)(CH_2CMe_3)(η^3-$CH_2CHCHPh$) (**4**), Cp*W(NO)(CH_2SiMe_3)(η^3-CH_2-$CHCHMe$) (**5**), and Cp*W(NO)(CH_2CMe_3)(η^3-CH_2CHCH_2) (**6**) have thus been synthesized in moderate yields. The solid-state molecular structures of **3**, **4**, **5**, and **6** feature $\sigma-\pi$ distorted allyl ligands in the endo conformation. Complex **1** effects the concurrent N−H and α-C−H activations of pyrrolidine and piperidine under ambient conditions and forms the alkyl amido complexes Cp*W(NO)(CH_2CMe_3)(NC_4H_7-2-$CMe_2CH{=}CH_2$) (**7**) and Cp*W(NO)(CH_2CMe_3)(NC_5H_9-2-$CMe_2CH{=}CH_2$) (**8**), respectively. Complexes **2**−**5** react with pyrrolidine in a similar manner, but the reaction of **3** to produce Cp*W(NO)(CH_2CMe_3)(NC_4H_7-2-$CH_2CMe{=}CH_2$) (**10**) is not as clean since **3** is thermally unstable at 20 °C. Unfortunately, the concurrent N−H and α-C−H activation transformation encompasses only a very limited range of substrates, namely cyclic amines. Complex **6**, which contains an unsubstituted allyl ligand, exhibits a unique mode of reactivity with pyrrolidine and piperidine, incorporating 2 equiv of the amines and forming Cp*W(NO)(NC_4H_8)($CHMeCH_2NC_4H_8$) (**13**) and Cp*W(NO)(NC_5H_{10})($CHMeCH_2NC_5H_{10}$) (**14**), respectively. Plausible mechanisms are suggested to account for the different modes of reactivity of the Cp*W(NO)(alkyl)(η^3-allyl) compounds with the cyclic amines. All new complexes have been characterized by conventional spectroscopic methods, and representative compounds have also been subjected to single-crystal X-ray crystallographic analyses.

Introduction

In recent years we have been investigating the family of Cp*M(NO)(hydrocarbyl)$_2$ compounds (Cp* = η^5-C_5Me_5; M = Mo, W) that exhibits hydrocarbyl-dependent thermal chemistry. Thus, gentle thermolysis of appropriate Cp*M(NO)(hydrocarbyl)$_2$ precursors results in the loss of hydrocarbon and the transient formation of 16e organometallic complexes such as Cp*M(NO)(alkylidene), Cp*M(NO)(η^2-acetylene), and Cp*M(NO)(η^2-benzyne). These intermediates first effect the single activation of hydrocarbon C−H bonds intermolecularly via the reverse of the transformations by which they were generated. Some of the new product complexes formed in this manner are stable and may be isolated. Others are thermally unstable under the experimental conditions employed and react further to effect double or triple C−H bond activations of the hydrocarbon substrates.[1] A particularly interesting member of the Cp*M(NO)(hydrocarbyl)$_2$ family of complexes is the alkyl allyl complex, Cp*W(NO)(CH_2CMe_3)(η^3-CH_2CHCMe_2) (**1**), that loses neopentane at 50 °C and forms two reactive 16e intermediate species. One intermediate is an η^2-allene complex, and the other is an η^2-diene complex, and both effect a variety of C−H bond activations, some of which are without precedent in the chemical literature.[2]

While extending our investigations of the thermal chemistry of Cp*W(NO)(CH_2CMe_3)(η^3-CH_2CHCMe_2) (**1**) to encompass various heteroatom-containing organic substrates, we subsequently discovered that it can also effect concurrent N−H and α-C−H activations of cyclic amines under ambient conditions without losing neopentane.[3] To the best of our knowledge, this type of transformation had not been reported previously.[4] We therefore decided to explore this chemistry more fully to establish the scope of these conversions as well as to acquire some insights as to the operative mechanism. This paper presents the results of those investigations. Specifically, we have synthesized and fully characterized five new Cp*W(NO)(alkyl)(η^3-allyl) complexes (**2**−**6**), and we have treated all six members of this family of compounds (i.e., **1**−**6**) with various amines to establish the generality of the concurrent N−H and α-C−H activation reactions first observed for **1**. A portion of this work has been previously communicated.[3]

Results and Discussion

Synthesis and Spectroscopic Properties of the Cp*W(NO)(alkyl)(η^3-allyl) Complexes. The six reactant compounds **1**–**6** can all be prepared in moderate yields via metathesis reactions

* Corresponding author. E-mail: legzdins@chem.ubc.ca.

(1) Pamplin, C. B.; Legzdins, P. *Acc. Chem. Res.* 2003, *36*, 223 andreferences cited therein.

(2) Ng, S. H. K.; Adams, C. S.; Hayton, T. W.; Legzdins, P.; Patrick, B. O. *J. Am. Chem. Soc.* **2003**, *125*, 15210.

(3) Tsang, J. Y. K.; Fujita-Takayama, C.; Buschhaus, M. S. A.; Patrick, B. O.; Legzdins, P. *J. Am. Chem. Soc.* **2006**, *128*, 14762.

(4) A related transformation is the N−H/C−H exchange of secondary amines catalyzed at high temperatures by homoleptic transition-metal dimethylamido complexes; see: Nugent, W. A.; Ovenall, D. W.; Holmes, S. J. *Organometallics* **1983**, *2*, 161.

10.1021/om701236k CCC: $40.75
Publication on Web 03/04/2008

Scheme 1

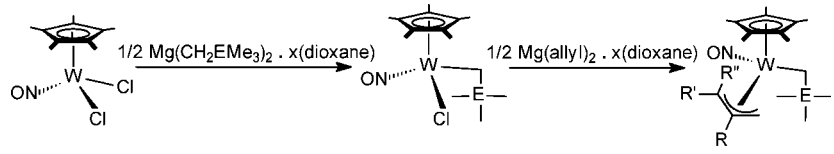

Complex	E	R	R'	R''	Color	Yield (%)
1	C	H	Me	Me	Orange	57
2	C	Me	H	H	Pale yellow	62
3	C	H	Me	H	Yellow-orange	43
4	C	H	Ph	H	Orange	58
5	Si	H	Me	H	Yellow-orange	65
6	C	H	H	H	Yellow	62

with magnesium reagents beginning with $Cp^*W(NO)Cl_2$, and they are all isolable as yellow to orange solids (Scheme 1). These compounds are formally 18e species; hence, it is not surprising that they are relatively stable toward oxygen and moisture in the crystalline state. For example, crystals of **2**, **4**, and **6** all maintain their luster for at least three months while exposed to air.

The solid-state molecular structures of compounds **3**, **4**, **5**, and **6** have all been established by X-ray crystallographic analyses, and these structures are shown in Figures 1 to 5, respectively. All four complexes feature allyl ligands that are in the endo conformation. It has been previously demonstrated by DFT calculations that the two different allyl conformations in Group 6 half-sandwich compounds of the type $Cp'ML_1L_2$(allyl) are very close in energy, with the endo form being slightly more stable.[5] In complex **3**, which contains the asymmetric 1-methylallyl ligand, the methyl substituent occupies a syn position on the allyl ligand and is cis to the smaller nitrosyl ligand, not to the bulkier neopentyl group. Complex **4** also crystallizes as a discrete isomer that features the phenyl substituent cis to the nitrosyl ligand. In contrast, complex **5** crystallizes as two isomers in a 2:1 ratio. The major isomer has a structure that is completely analogous to that of **3**. On the other hand, the minor isomer is a coordination isomer that features the methyl substituent of the 1-methylallyl ligand on the opposite end, cis to the CH_2SiMe_3 group (Figure 4). As expected, the allyl ligands of all the complexes exhibit a $\sigma-\pi$ distortion (i.e., the C−C linkage trans to the nitrosyl group is shorter and has a higher multiple-bond character than the C−C

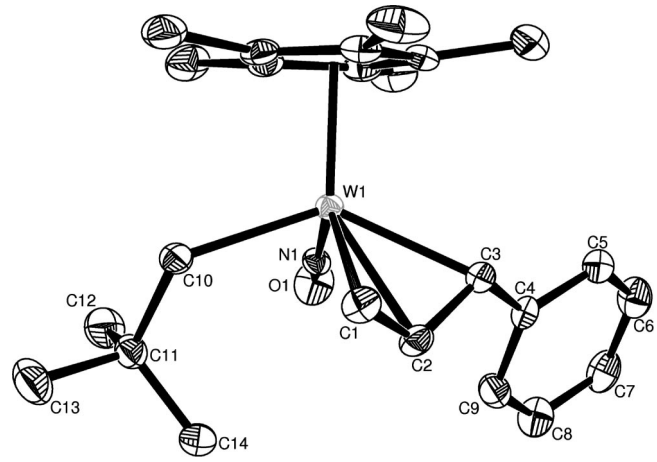

Figure 2. Solid-state molecular structure of **4** with 50% probability thermal ellipsoids. Selected interatomic distances (Å) and angles (deg): W(1)−C(1) = 2.397(3), W(1)−C(2) = 2.345(3), W(1)−C(3) = 2.304(3), W(1)−C(10) = 2.265(3), W(1)−N(1) = 1.772(3), N(1)−O(1) = 1.223(4), C(1)−C(2) = 1.365(5), C(2)−C(3) = 1.437(5), C(3)−C(4) = 1.494(4), C(1)−C(2)−C(3) = 120.9(3), C(2)−C(3)−C(4) = 121.0(3), W(1)−C(10)−C(11) = 123.6(2), W(1)−N(1)−O(1) = 169.7(2).

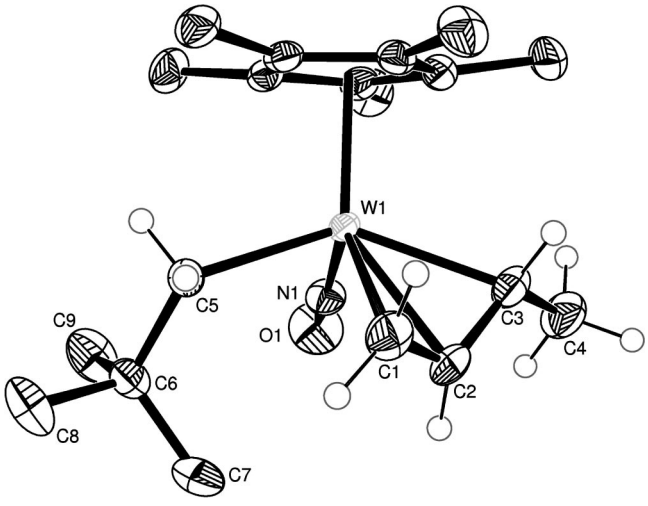

Figure 1. Solid-state molecular structure of **3** with 50% probability thermal ellipsoids. Selected interatomic distances (Å) and angles (deg): W(1)−C(1) = 2.401(3), W(1)−C(2) = 2.346(3), W(1)−C(3) = 2.282(3), W(1)−C(5) = 2.257(3), W(1)−N(1) = 1.764(2), N(1)−O(1) = 1.221(3), C(1)−C(2) = 1.372(5), C(2)−C(3) = 1.425(4), C(3)−C(4) = 1.509(4), C(1)−C(2)−C(3) = 119.3(3), C(2)−C(3)−C(4) = 120.4(3), W(1)−C(5)−C(6) = 123.4(2), W(1)−N(1)−O(1) = 170.5(2).

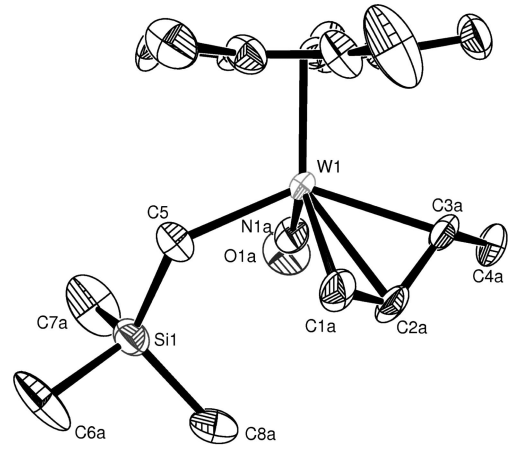

Figure 3. Solid-state molecular structure of the major isomer of **5** with 50% probability thermal ellipsoids. Selected interatomic distances (Å) and angles (deg): W(1)−C(1a) = 2.44(1), W(1)−C(2a) = 2.339(10), W(1)−C(3a) = 2.278(8), W(1)−C(5) = 2.212(6), W(1)−N(1a) = 1.690(8), N(1a)−O(1a) = 1.210(11), C(1a)−C(2a) = 1.392(16), C(2a)−C(3a) = 1.415(16), C(3a)−C(4a) = 1.504(14), C(1a)−C(2a)−C(3a) = 118.0(11), C(2a)−C(3a)−C(4a) = 119.3(10), W(1)−C(5)−Si(1) = 119.4(4), W(1)−N(1a)−O(1a) = 167.5(10).

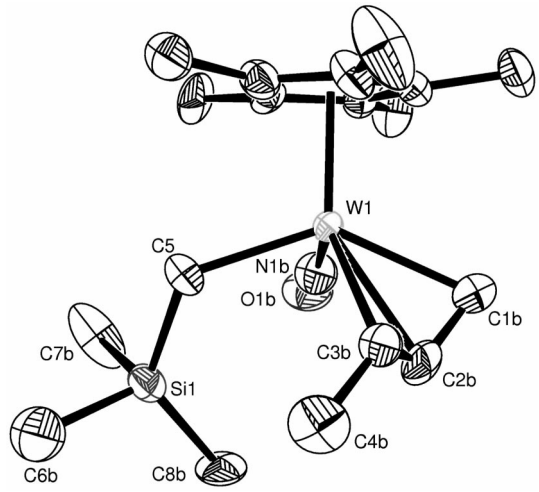

Figure 4. Solid-state molecular structure of the minor isomer of **5** with 50% probability thermal ellipsoids. Selected interatomic distances (Å) and angles (deg): W(1)−C(1b) = 2.35(3), W(1)−C(2b) = 2.39(2), W(1)−C(3b) = 2.41(3), W(1)−C(5) = 2.212(6), W(1)−N(1b) = 1.863(15), N(1)−O(1b) = 1.275(17), C(1b)−C(2b) = 1.40(2), C(2b)−C(3b) = 1.41(2), C(3b)−C(4b) = 1.50(2), C(1b)−C(2b)−C(3b) = 118(3), C(2b)−C(3b)−C(4b) = 120(3), W(1)−C(5)−Si(1) = 119.4(4), W(1)−N(1b)−O(1b) = 171(2).

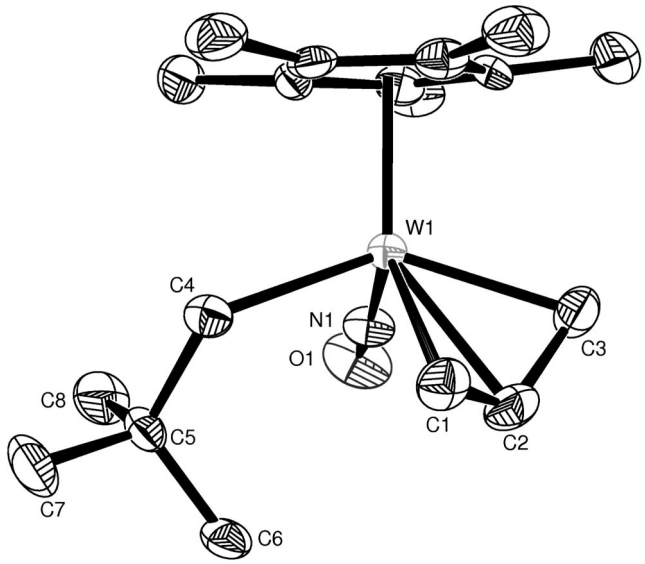

Figure 5. Solid-state molecular structure of **6** with 50% probability thermal ellipsoids. Selected interatomic distances (Å) and angles (deg): W(1)−C(1) = 2.416(6), W(1)−C(2) = 2.339(6), W(1)−C(3) = 2.252(6), W(1)−C(5) = 2.267(6), W(1)−N(1) = 1.770(5), N(1)−O(1) = 1.236(7), C(1)−C(2) = 1.361(10), C(2)−C(3) = 1.425(10), C(1)−C(2)−C(3) = 118.3(7), W(1)−C(5)−C(6) = 124.3(4), W(1)−N(1)−O(1) = 171.2(5).

bond cis to nitrosyl), a manifestation of the electronic asymmetry extant at the metal centers.[6–10]

The ^{1}H NMR spectroscopic data for all the Cp*W(NO)(alkyl)(η^3-allyl) complexes **1**−**6** are very similar. The data indicate that their solid-state molecular structures persist in solution, and in general the signals attributable to the protons of the allyl ligands are typical for organometallic allyl complexes. For complexes **3** and **5**, a second set of proton signals, attributable to their respective minor isomers, are observable, and these signals are listed in the Experimental Section. Nevertheless, the minor isomer of compound **3** apparently does not cocrystallize with the isolated major isomer. Complex **4** does not exhibit stereoisomerism, most likely because the allyl phenyl substituent is too bulky to be situated cis to the even bulkier neopentyl ligand. Furthermore, the ^{13}C NMR data for **1**−**6** support the fact that allyl $\sigma-\pi$ distortions persist in solution. Specifically, the chemical shifts for the σ-terminal allyl carbon signals (ca. 40 ppm when unsubstituted) are some 35 ppm upfield from those of the π-terminal allyl carbons (ca. 75 ppm when unsubstituted). The middle carbon signals appear in the vicinity of 110 ppm when the carbon is unsubstituted.

The ^{1}H NMR spectra of several of the Cp*W(NO)(alkyl)(η^3-allyl) compounds have been acquired at both high and low temperatures in order to investigate structural isomerism in solution. The spectral results indicate that the solution structures are essentially static, that endo−exo isomerism is not present, and that isomers featuring the asymmetric allyl ligand $CH_2CHCHMe$ do not interconvert on the NMR time scale. For example, the ^{1}H NMR spectrum of complex **6** in acetone-d_6 remains essentially unchanged over the temperature range from +20 to −75 °C. The ^{1}H NMR spectrum of the same compound at 70 °C in C_6D_6 is identical with the room temperature spectrum. Similarly, in a series of low-temperature ^{1}H NMR spectra of complex **5** in $CDCl_3$, the allyl signals due to the minor isomer begin to sharpen as the temperature falls near −15 °C, but there is no observable peak shifting or coalescing.

Thermal Stabilities of the Cp*W(NO)(alkyl)(η^3-allyl) Complexes. The new compounds **2**−**6** have been heated in various organic solvents to establish their thermal properties. On the basis of the documented thermal properties of **1** (i.e., loses neopentane at 50 °C), it was anticipated at the outset that the presence of a meso-hydrogen or a terminal methyl group on the allyl ligand would lead to thermal reactivity of the metal complex. Thermolysis reactions confirm that this expectation is true for the most part, except for complex **6**, which appears to be stable at 70 °C in both C_6D_6 and PMe_3 for 16 h. The reason for this thermal stability is unclear at this point. Complex **2**, which has neither a meso proton nor a terminal methyl group, also remains unchanged after being heated at 70 °C for 16 h in C_6D_6. On the other hand, complex **3** proves to be unstable even at room temperature, decomposing in the solid state into a brown intractable solid over 64 h. In solution it decomposes completely during 1 d at 20 °C. Complex **4** as a crystalline solid is stable at room temperature for at least a few months (vide infra), but in solution at 75 °C it is consumed within 1 d. Complex **5** is also thermally stable at 20 °C, but loses $SiMe_4$ in solution at 70 °C also over the course of 1 d.

Reactions of the Cp*W(NO)(alkyl)(η^3-allyl) Complexes with Cyclic Amines. (A) Cp*W(NO)(CH_2CMe_3)(η^3-CH_2-$CHCMe_2$) (1). Treatment of **1** with neat pyrrolidine at room temperature results in the quantitative formation of the alkyl amido complex, **7** (Scheme 2).

Compound **7** is very soluble in common organic solvents, but it can be isolated as an orange air-stable solid in 52% yield by chromatography of the final reaction mixture on alumina with pentane as eluant and crystallization from the concentrated eluate at −30 °C. Its solid-state molecular structure (Figure 6)

(5) Schilling, B. E. R.; Hoffmann, R.; Faller, J. W. *J. Am. Chem. Soc.* **1979**, *101*, 592.
(6) Bent, H. A. *Chem. Rev.* **1961**, *61*, 275.
(7) Ipaktschi, J.; Mirzaei, F.; Demuth-Eberle, G. J.; Beck, J.; Serafin, M. *Organometallics* **1997**, *16*, 3965.
(8) Frohnapfel, D. S.; White, P. S.; Templeton, J. *Organometallics* **1997**, *16*, 3737.
(9) Villanueva, L. A.; Ward, Y. D.; Lachicotte, R.; Liebeskind, L. S. *Organometallics* **1996**, *15*, 4190.
(10) Adams, R. D.; Chodosh, D. F.; Faller, J. W.; Rosan, A. M. *J. Am. Chem. Soc.* **1979**, *101*, 2570.

Scheme 2

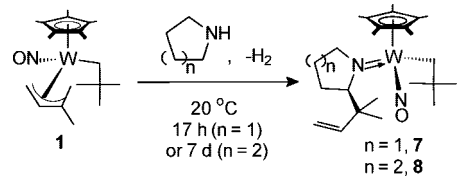

exhibits metrical parameters that are consistent with solution NMR data and reflect loss of hydrogen atoms from the pyrrolidine nitrogen atom, N(2), and a carbon atom α to it, C(9). The W(1)−N(2) bond length of 1.940(2) Å and the coplanarity of W(1), N(2), C(6), and C(9) in **7** are indicative of this linkage being a slightly elongated W=N double bond,[11] the tungsten center thereby attaining the favored 18e configuration. The original allyl ligand in **1** has become a vinylalkyl substituent at C(9) of the newly formed pyrrolide ligand in **7**. Once formed, complex **7** (mp 115 °C) is thermally stable, and undergoes no detectable changes when maintained at 120 °C for 1 h.

In a similar manner, treatment of **1** with piperidine under ambient conditions affords orange complex **8**, the product analogous to **7**, as the principal organometallic compound (Scheme 2). However, the reaction proceeds more slowly than with pyrrolidine, and so it is accompanied by some thermal decomposition of the reactant **1**. Workup of the final reaction mixture in a manner analogous to that employed for the isolation of **7** affords **8** in 17% yield. Complex **8** is also very soluble in common organic solvents. The solid-state molecular structure of **8** (Figure 7) bears a striking resemblance to that exhibited by **7**, and its spectroscopic properties confirm that this structure persists in solutions.

Unfortunately, the concurrent N−H and α-C−H activation transformation encompasses only a very limited range of substrates. As noted above, piperidine reacts with complex **1** to form the concurrent N−H and α-C−H activation product, namely, Cp*W(NO)(CH_2CMe_3)(NC_5H_9-2-$CMe_2CH{=}CH_2$) (**8**). However, other amines, such as aniline, cyclohexylamine, diethylamine, and *tert*-butylamine, are all unreactive in this regard.

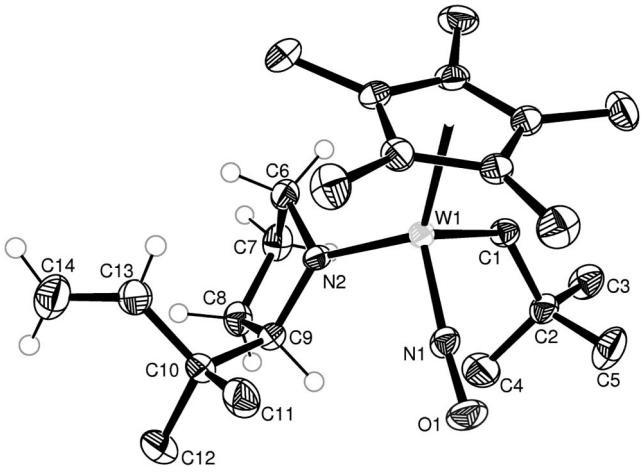

Figure 6. Solid-state molecular structure of **7** with 50% probability thermal ellipsoids shown. Selected interatomic distances (Å) and angles (deg): W(1)−N(2) = 1.940(2), N(2)−C(6) = 1.485(3), N(2)−C(9) = 1.496(4), C(9)−C(10) = 1.560(4), C(10)−C(13) = 1.510(4), C(13)−C(14) = 1.316(4), W(1)−N(1) = 1.761(2), N(1)−O(1)=1.239(3),W(1)−N(1)−O(1)=169.4(2),C(10)−C(13)−C(14) = 127.4(3), C(9)−C(10)−C(13) = 111.2(2), N(1)−W(1)−N(2) = 98.61(10), N(1)−W(1)−C(1) = 98.41(11), W(1)−N(2)−C(6) = 119.91(18), C(6)−N(2)−C(9) = 106.1(2), W(1)−N(2)−C(9) = 132.32(17).

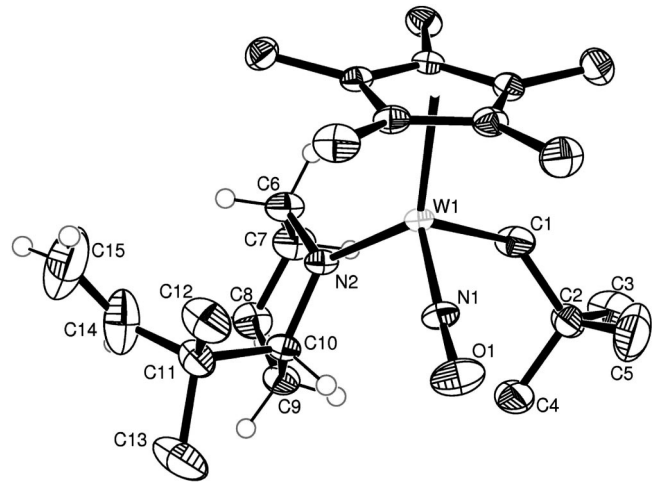

Figure 7. Solid-state molecular structure of **8** with 50% probability thermal ellipsoids shown. Selected interatomic distances (Å) and angles (deg): W(1)−N(2) = 1.937(2), N(2)−C(6) = 1.482(3), N(2)−C(10) = 1.480(3), C(10)−C(11) = 1.573(4), C(11)−C(14) = 1.494(5), C(14)−C(15) = 1.306(6), W(1)−N(1) = 1.753(2), N(1)−O(1)=1.229(3),W(1)−N(1)−O(1)=169.3(2),C(11)−C(14)−C(15) = 127.8(5), C(10)−C(11)−C(14) = 114.1(3), N(1)−W(1)−N(2) = 97.76(9), N(1)−W(1)−C(1) = 97.38(10), W(1)−N(2)−C(6) = 118.38(16), C(6)−N(2)−C(10) = 113.9(2), W(1)−N(2)−C(10) = 127.64(16).

(B)Complexes 2–5. Four of the other Cp*W(NO)(alkyl)(η³-allyl) complexes, namely **2**−**5**, react with pyrrolidine under ambient conditions in a manner similar to that described above for **1**. Thus, treatment of complex **2** with pyrrolidine at room temperature for 64 h leads to the formation of two new complexes, one of which is Cp*W(NO)(CH_2CMe_3)(NC_4H_7-2-$CH_2CMe{=}CH_2$) (**9**). The reaction is sluggish and does not go to completion before significant product degradation occurs. Complex **9** can be obtained in low yields by fractional crystallization from pentane after extraction from the less soluble unreacted starting material following chromatography of the final reaction mixture on alumina. The solid-state molecular structure of **9** is shown in Figure 8, and its metrical parameters closely resemble those of **7** (Figure 6). There is also a second product formed in a ca. 1:2 ratio vs. **9** according to the integration of their respective ^{1}H NMR Cp* methyl peaks. However, this product has not yet been identified since it decomposes upon chromatography on alumina.

Complex **3** also reacts with pyrrolidine to form the concurrent N−H and α-C−H activation product, Cp*W(NO)(CH_2CMe_3)-(NC_4H_7-2-$CHMeCH{=}CH_2$) (**10**). As in the case of complex **2**, the reaction is not clean. This feature may well reflect the fact that complex **3** also possesses thermal reaction pathways that could, for example, lead to the simple C−H activation on the pyrrolidine CH_2 backbone.[12] In any event, complex **10** can be isolated as the sole organometallic product after chromatography on alumina. Notably, complexes **4** and **5**, which are thermally stable at room temperature, produce the cleanest reactions. Both compounds Cp*W(NO)(CH_2CMe_3)(NC_4H_7-2-$CHPhCH{=}CH_2$) (**11**) and Cp*W(NO)(CH_2SiMe_3)(NC_4H_7-2-$CHMeCH{=}CH_2$) (**12**) are formed quantitatively after 16 h and 4 d, respectively, at ambient temperatures as judged by ^{1}H NMR spectroscopy.

(11) A search of the Cambridge Structural Database reveals that typical W=N bond lengths fall between 1.70 and 1.80 Å.

(12) Tsang, J. Y. K.; Buschhaus, M. S. A.; Legzdins, P. *J. Am. Chem. Soc.* **2007**, *129*, 5372.

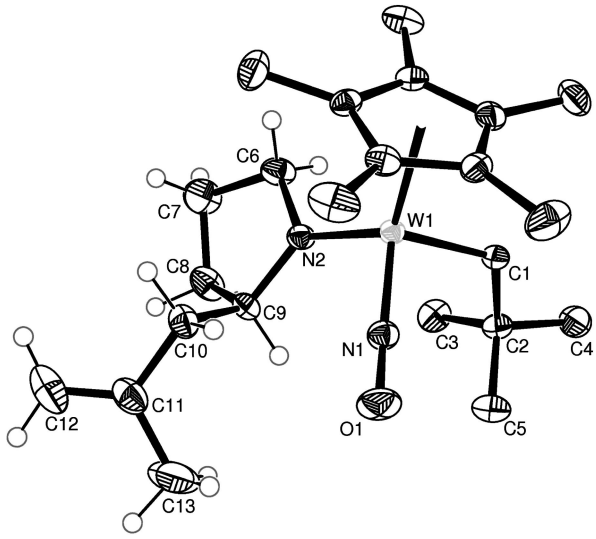

Figure 8. Solid-state molecular structure of **9** with 50% probability thermal ellipsoids. Selected interatomic distances (Å) and angles (deg): W(1)−C(1) = 2.184(3), W(1)−N(2) = 1.938(2), W(1)−N(1) = 1.763(2), N(1)−O(1) = 1.239(3), C(11)−C(12) = 1.324(5), C(10)−C(11)−C(12) = 121.6(4), W(1)−N(2)−C(9) = 127.17(18), W(1)−N(2)−C(6) = 124.65(18), W(1)−N(1)−O(1) = 168.7(2).

Like **1**, compounds **2**−**5** are also unreactive toward other amines such as aniline, cyclohexylamine, diethylamine, and *tert*-butylamine.

Mechanistic Insights on the Concurrent N−H and α-C−H Activation Process. The reaction between **2** and pyrrolidine has been monitored by ^{1}H NMR spectroscopy to gain some mechanistic insights concerning the general reaction. Unfortunately, no organometallic intermediates are observable. Interestingly, the ^{1}H NMR spectrum of the volatiles from the reaction contains a small singlet at 4.80 ppm, indicative of the production of H_2 during the course of the reaction. This chemical shift has been confirmed by recording the ^{1}H NMR spectrum of a separately prepared sample of H_2 in pyrrolidine in a J. Young NMR tube equipped with a C_6D_6 capillary.

Since all the product complexes are formed at room temperature, it is unlikely that the allyl reactants convert to an η^2-allene- or an η^2-diene-containing intermediate[2] or that the pyrrolidine is dehydrogenated to pyrroline prior to reacting.[13] Nevertheless, a number of possible mechanisms can be envisaged for these conversions, and more studies will be required to evaluate the various possibilities. Particularly intriguing in this regard is the fact that the allyl, and not the alkyl, groups migrate with such selectivity. A possible reaction mechanism, involving an $\eta^3 \rightarrow \eta^1$ interconversion of the allyl ligand, the coordination of pyrrolidine, and a subsequent metal-mediated rearrangement resulting in the elimination of H_2, is proposed in Scheme 3.

Precedent for the allyl ligand undergoing such an $\eta^3 \rightarrow \eta^1$ interconversion and then an intramolecular migration is provided by the reaction of Cp*W(NO)(CH_2SiMe_3)(η^3-$CH_2CHCHMe$) (**5**) with CNPh that results in the clean formation of Cp*W(NO)(CH_2SiMe_3)(η^2-$CH_3CH{=}CHCH_2C{=}NPh$) (Scheme 4).[14]

Reactions of Cp*W(NO)(CH_2CMe_3)(η^3-C_3H_5) (6) with Cyclic Amines. Of the six Cp*W(NO)(alkyl)(η^3-allyl) complexes studied, only the one containing an unsubstituted allyl ligand (i.e., **6**) exhibits a unique mode of reactivity with pyrrolidine and piperidine. Thus, when complex **6** is treated with pyrrolidine at room temperature, orange Cp*W(NO)(NC_4H_8)($CHMeCH_2NC_4H_8$) (**13**) is formed as the only organometallic product (Scheme 5). The reaction is deemed to be complete within 5 h, and prolonged reaction times lead to reduced yields. Complex **13** is not amenable to chromatography on alumina, but can be obtained analytically pure by crystallization from pentane as fibrous needles. X-ray quality crystals result from recrystallization of these needles from Et_2O, and a crystallographic analysis affords the solid-state molecular structure of **13** shown in Figure 9. As can be seen in this figure, 2 equiv of pyrrolidine have been incorporated during the chemical transformation, the neopentyl ligand has been lost, and what had been the allyl ligand has now become a pyrrolidyl-isopropyl entity.

It is not clear at present why complex **6** reacts differently with pyrrolidine than do the other allyl complexes (vide supra). Nevertheless, a plausible mechanism can be proposed for the overall conversion, and it is depicted in Scheme 6. First, the allyl ligand undergoes nucleophilic attack by pyrrolidine on the terminal carbon trans to the nitrosyl.[15] It is well-established that nucleophilic attack on bound allyls in Group 6

Scheme 3

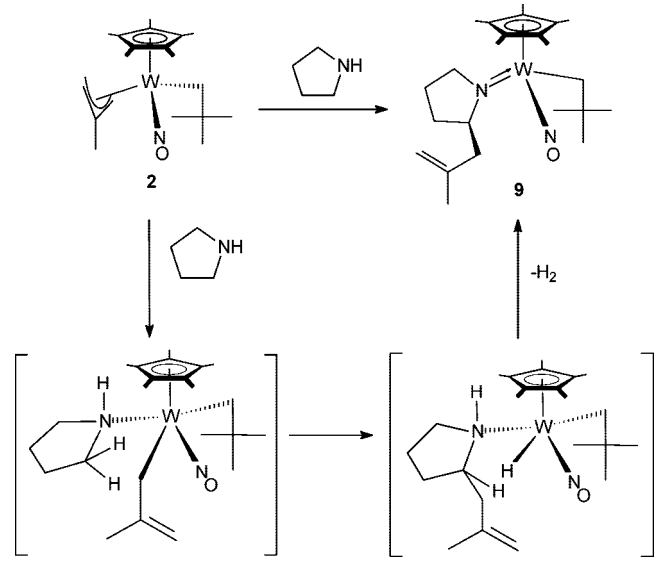

Scheme 4

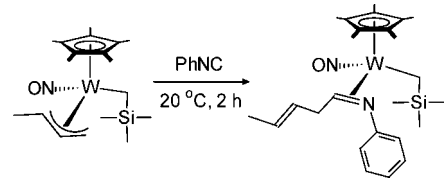

Scheme 5

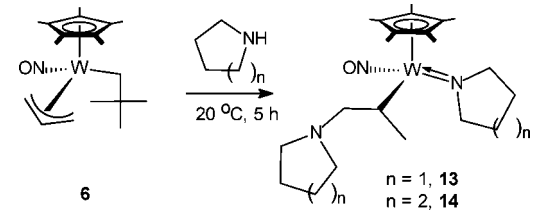

(13) For a review of methods for the synthesis of Δ^1-pyrrolines, see: Shvekhgeimer, M.-G. A. *Chem. Heterocycl. Compd.* **2003**, *39*, 405.

(14) Graham, P. M.; Semproni, S. P.; Legzdins, P. Unpublished observations.

(15) For a recent example of this type of transformation, see: Amatore, C.; Genin, E.; Jutand, A.; Mensah, A. *Organometallics* **2007**, *26*, 1875.

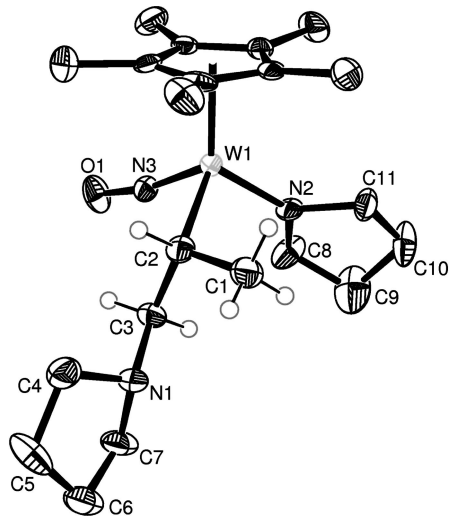

Figure 9. Solid-state molecular structure of **13** with 50% probability thermal ellipsoids. Selected interatomic distances (Å) and angles (deg): W(1)−C(2) = 2.198(6), W(1)−N(2) = 1.926(4), W(1)−N(3) = 1.749(5), N(3)−O(1) = 1.246(5), C(1)−C(2) = 1.537(7), C(2)−C(3) = 1.544(6), C(3)−N(1) = 1.462(7), C(1)−C(2)−C(3) = 110.0(4), C(2)−C(3)−N(1) = 114.3(5), C(3)−N(1)−C(4) = 114.0(4), C(3)−N(1)−C(7) = 112.9(5), W(1)−N(2)−C(8) = 128.7(3), W(1)−N(2)−C(11) = 125.1(3), W(1)−N(3)−O(1) = 168.8(4).

Scheme 6

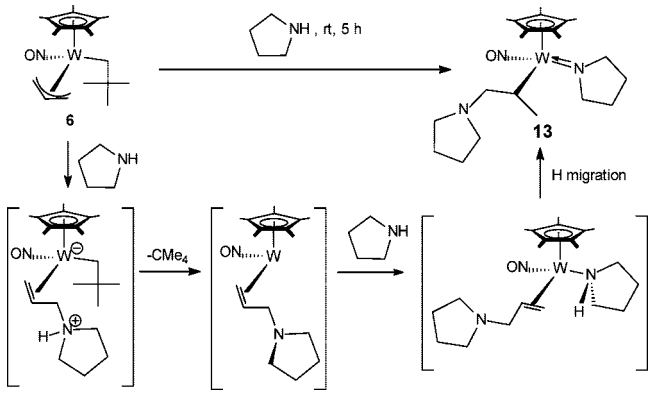

half-sandwich compounds of this type[10,16] occurs trans to the better π-acceptor (i.e., the NO ligand) when the allyl is in the endo conformation.[5] Next, the neopentyl group is liberated by internal protonation, and a neutral, coordinatively unsaturated metal center is formed. Finally, a second molecule of pyrrolidine coordinates to the metal center and yields **13** after intramolecular proton migration.

In a similar manner, piperidine reacts with **6** at room temperature to form Cp*W(NO)(NC_5H_{10})($CHMeCH_2NC_5H_{10}$) (**14**) (Scheme 5). The reaction time required is much longer (2 d), and consequently a considerable amount of **14** decomposes before **6** is completely consumed, thereby accounting for the lower yield of the reaction. However, just like the other Cp*W(NO)(alkyl)(η^3-allyl) complexes **1**−**5**, complex **6** remains unchanged when it is dissolved in aniline, cyclohexylamine, diethylamine or *tert*-butylamine for 1 d at 20 °C.

Epilogue

During our investigations of these six allyl complexes, we have discovered that the presence of a meso hydrogen on the allyl ligand is not the only requirement for the complex to exhibit thermal reactivity. Other factors, such as steric factors, can render the loss of neopentane more facile, as in the cases of complexes **4** vs **6**. On the other hand, the presence of a methyl group does lead to thermal reactivity of the compounds, presumably because of the possibility of β-hydrogen elimination by a 16e complex as it undergoes allyl $\eta^3 \rightarrow \eta^1$ interconversion. The reactivity with cyclic amines also depends on the sterics of the allyl ligand. Concurrent N−H and α-C−H activation occurs readily when the allyl ligand is sterically demanding, as in the cases of complexes **1**, **3**, **4**, and **5**, and thus able to undergo $\eta^3 \rightarrow \eta^1$ interconversion more readily. In the intermediate case of complex **2** concurrent N−H and α-C−H activation is sluggish, and for **6**, the complex with the smallest allyl ligand, only traditional nucleophilic attack by the cyclic amines occurs. Such an attack is also expected to be less likely electronically for those complexes containing allyl ligands with electron-donating methyl substituents.

Experimental Section

General Methods. All reactions and subsequent manipulations involving organometallic reagents were performed under anaerobic and anhydrous conditions either under high vacuum or an inert atmosphere of prepurified dinitrogen. Purification of inert gases was achieved by passing them first through a column containing MnO and then a column of activated 4 Å molecular sieves. Conventional glovebox and vacuum-line Schlenk techniques were utilized throughout. The gloveboxes employed were Innovative Technologies Lab-Master 100 and MS-130 BG dual-station models equipped with freezers maintained at − 30 °C. Most of the reactions were performed in thick-walled glass vessels possessing Kontes greaseless stopcocks and sidearm inlets for vacuum-line attachment. Small-scale reactions and NMR spectroscopic analyses were conducted in J. Young NMR tubes which were also equipped with Kontes greaseless stopcocks. All solvents were dried with appropriate drying agents under a dinitrogen atmosphere and were distilled prior to use, or they were transferred directly under vacuum from the appropriate drying agent. Hydrocarbon solvents, diethyl ether, and tetrahydrofuran were dried and distilled from sodium benzophenone ketyl. Commercially available (C_3H_5)MgCl (Aldrich, 1.0 M in THF), (CH_2CMeCH_2)MgCl (Aldrich, 0.5 M in THF), and ($CH_2CHCHMe$)MgCl (Aldrich, 0.5 M in THF) were transformed into the corresponding diallylmagnesium reagents in the usual manner.[17,18] Cp*W(NO)(CH_2CMe_3)Cl[19] and Cp*W(NO)(CH_2SiMe_3)Cl[20] were prepared according to published procedures. The synthesis of ($CH_2CHCHPh$)MgCl from cinnamyl chloride (Aldrich) and magnesium (Strem) was carried out in a manner similar to that described previously for the synthesis of other allylmagnesium reagents,[2] and it was converted into the bis(allyl)-magnesium reagent in the usual manner.[17,18] The progress of most reactions was monitored by NMR spectroscopy, but the isolated yields of all new complexes have not been optimized.

(16) Nucleophilic attack on a metal-bound allyl ligand is a very common reaction type for related Cp′MoL_2(allyl) complexes, see:(a) Vanarsdale, W. E.; Winter, R. E. K.; Kochi, J. K. *Organometallics* **1986**, *5*, 645. (b) Faller, J. W.; Murray, H. H.; White, D. L.; Chao, K. H. *Organometallics* **1983**, *2*, 400. (c) Pearson, A. J.; Khan, Md. N. I.; Clardy, J. C.; Cunheng, H. *J. Am. Chem. Soc.* **1985**, *107*, 2748.

(17) Debad, J. D.; Legzdins, P.; Batchelor, R. J.; Einstein, F. W. B. *Organometallics* **1993**, *12*, 2094.

(18) There were instances when the isolation of the bis(allyl)magnesium reagent was unsuccessful, such as when removal of solvent left behind an intractable oily material. In such cases the oily residue was redissolved in Et_2O, and the solution was used as such after the concentration of the allylating reagent had been established by an HCl titration. The Et_2O solution was stored in a resealable glass bomb.

(19) Dryden, N. H.; Legzdins, P.; Einstein, F. W. B.; Jones, R. H. *Can. J. Chem.* **1988**, *66*, 2100.

(20) Debad, J. D.; Legzdins, P.; Batchelor, R. J.; Einstein, F. W. B. *Organometallics* **1992**, *11*, 6.

Table 1. X-ray Crystallographic Data for Complexes 3, 4, 5, 6, 7, 8, 9 and 13

	3	4	5	6	7	8	9	13
crystal data								
empirical formula	$C_{19}H_{33}NOW$	$C_{24}H_{35}NOW$	$C_{18}H_{33}NOSiW$	$C_{18}H_{31}NOW$	$C_{24}H_{42}N_2OW$	$C_{25}H_{44}N_2OW$	$C_{23}H_{40}N_2OW$	$C_{21}H_{37}N_3OW$
crystal habit, color	prism, yellow	rod, yellow-orange	prism, orange	prism, orange	needle, orange	prism, yellow	prism, yellow	needle, yellow
crystal size (mm)	0.45 × 0.30 × 0.20	1.4 × 0.1 × 0.1	0.8 × 0.5 × 0.5	0.35 × 0.22 × 0.10	0.20 × 0.10 × 0.05	0.35 × 0.30 × 0.25	0.40 × 0.175 × 0.075	0.55 × 0.075 × 0.05
crystal system	monoclinic	monoclinic	monoclinic	monoclinic	monoclinic	monoclinic	monoclinic	triclinic
space group	$P2_1/c$	$P2_1/c$	$P2_1/c$	$P2_1/c$	$P2_1/n$	$P2_1/n$	$P2_1/c$	P_{-1}
volume (Å^3)	1940.63(8)	2223.15(17)	1997.7(5)	1837.54(17)	2418.6(8)	2597.4(4)	2347.98(14)	2217.0(6)
a (Å)	9.0412(2)	12.7252(6)	9.4739(14)	10.6510(6)	11.732(3)	10.776(1)	12.6452(4)	8.0022(10)
b (Å)	14.2430(3)	11.7231(5)	13.991(2)	11.5052(6)	13.594(2)	18.681(2)	8.1081(3)	16.383(3)
c (Å)	15.6092(4)	15.2438(7)	15.631(2)	15.1007(8)	15.641(3)	13.048(1)	22.9995(8)	17.082(3)
α (deg)	90	90	90	90	90	90	90	84.451(6)
β (deg)	105.103(1)	102.146(2)	105.378(7)	96.778(3)	104.161(8)	98.560(5)	95.311(2)	89.925(6)
γ (deg)	90	90	90	90	90	90	90	84.088(6)
Z	4	4	4	4	4	4	4	4
density (calcd) (Mg/m^3)	1.627	1.606	1.634	1.667	1.534	1.464	1.540	1.592
abs coeff (mm^{-1})	5.955	5.209	5.845	6.286	4.792	4.464	4.934	5.224
F_{000}	944	1072	976	912	1128	1160	1096	1064
data collection and refinement								
measd reflns: total	29663	27675	33457	5306	159755	60650	36666	11672
measd reflns: unique	4599	5262	5957	5306	12520	6277	5392	11672
final R indices[a]	R1 = 0.0178, wR2 = 0.0423	R1 = 0.0210, wR2 = 0.0660	R1 = 0.0456, wR2 = 0.1103	R1 = 0.0304, wR2 = 0.1024	R1 = 0.043, wR2 = 0.067	R1 = 0.0201, wR2 = 0.0502	R1 = 0.0200, wR2 = 0.0500	R1 = 0.0315, wR2 = 0.0553
goodness-of-fit on F^2[b]	1.080	1.153	1.181	1.106	0.938	1.065	1.061	0.883
largest diff peak and hole (e$^-$Å^{-3})	1.185 and −0.806	1.504 and −1.371	5.310 and −7.005	1.259 and −1.351	1.869 and −1.156	1.909 and −1.093	1.731 and −0.674	1.925 and −0.957

[a] R1 on $F = \sum(||F_o| - |F_c||)/\sum|F_o|$ ($I > 2\sigma(I)$); wR2 = $[(\sum(F_o^2 - F_c^2)^2)/\sum w(F_o^2)^2]^{1/2}$ (all data); $w = [\sigma^2 F_o^2]^{-1}$. [b] GOF = $[\sum(w(|F_o| - |F_c|)^2/\text{degrees of freedom}]^{1/2}$.

All IR samples were prepared as Nujol mulls, and their spectra were recorded on a Thermo Nicolet 4700 FT-IR spectrometer. NMR spectra were recorded at room temperature on Bruker AV-300, AV-400, or AMX-500 spectrometers. All chemical shifts are reported in ppm, and all coupling constants are reported in Hz. ^{1}H NMR spectra are referenced to the residual protio isotopomer present in a particular solvent, and ^{13}C NMR spectra are referenced to the natural-abundance carbon signal of the solvent employed. Where necessary, ^{1}H−^{1}H COSY, ^{1}H−^{13}C HMQC, ^{1}H−^{13}C HMBC, and ^{13}C APT experiments were carried out to correlate and assign ^{1}H and ^{13}C NMR signals. Low-resolution mass spectra (EI, 70 eV) were recorded by the staff of the UBC mass spectrometry facility with a Kratos MS-50 spectrometer. Elemental analyses were performed by Mr. Minaz Lakha of the UBC microanalytical facility.

Preparation of Cp*W(NO)(CH$_2$CMe$_3$)(η³-CH$_2$CHCMe$_2$) (1). In a glovebox, a 100-mL Schlenk tube was charged with a magnetic stir bar and Cp*W(NO)(CH$_2$CMe$_3$)Cl (483 mg, 1.15 mmol). A 400-mL Schlenk tube was then charged with a magnetic stir bar and the dimethylallyl magnesium reagent (147 mg, 1.16 mmol). On a vacuum line, Et$_2$O (200 mL) from a bomb was cannulated into the Schlenk tube containing the magnesium reagent with vigorous stirring to ensure its dissolution. The resulting colorless solution was then frozen by cooling to −196 °C with a liquid N$_2$ bath. Et$_2$O (50 mL) was added in a similar fashion to the Schlenk tube containing the solid Cp*W(NO)(CH$_2$CMe$_3$)Cl to obtain a purple solution that was then cooled to −60 °C with a dry ice/acetone bath. The purple solution was then cannulated dropwise into the 400-mL Schlenk tube (maintained at −196 °C) at a slow enough rate that allowed the added solution to freeze upon contact with the solidified ethereal solution of the magnesium reagent. Sufficient Et$_2$O was added to the 100-mL Schlenk tube and subsequently cannulated into the reaction flask to ensure complete transfer of Cp*W(NO)(CH$_2$CMe$_3$)Cl. The liquid N$_2$ bath was replaced with a liquid N$_2$/acetone bath at −60 °C to enable the ethereal contents to melt slowly. After being stirred for 5 min, the purple solution changed to a straw-yellow color, which then became a turbid orange after a further 10 min. The solution was stirred at −60 °C for a total of 45 min, whereupon the contents were warmed to room temperature to ensure completion of the reaction. The volume of the mixture was reduced under vacuum to ∼100 mL, and the turbid orange solution was filtered through an alumina(I) column (2 × 3 cm), which was also rinsed with fresh Et$_2$O (2 × 10 mL), to obtain a clear bright orange filtrate. The volatiles were then removed from the filtrate in vacuo to obtain an orange crystalline powder that was dried at room temperature under high vacuum for 1 h. Analysis of this solid by ^{1}H NMR spectroscopy revealed that complex **1** was the sole organometallic product. Analytically pure **1** was obtained as orange microcrystals (296 mg, 57%) via crystallization from a THF/hexanes mixture (5 mL/20 mL) at −25 °C.

1: IR (cm^{-1}) 1546 (s, ν_{NO}). MS (LREI, *m/z*, probe temperature 150 °C) 489 [P$^+$, ^{184}W]. ^{1}H NMR (300 MHz, C$_6$D$_6$) δ 0.67 (s, 3H, allyl Me), 1.02 (obs, 1H, Npt CH$_2$), 1.02 (s, 3H, allyl Me), 1.42 (s, 9H, Npt CMe$_3$), 1.42 (obs, 1H, allyl CH$_2$), 1.53 (s, 15H, C$_5$Me$_5$), 2.69 (m, 1H, allyl CH$_2$), 4.45 (m, 1H, allyl CH). ^{1}H NMR (400 MHz, CD$_2$Cl$_2$) δ 0.88 (d, $^2J_{HH}$ = 14.2, 1H, Npt CH$_2$), 0.99 (s, 3H, allyl Me), 1.02 (d, $^2J_{HH}$ = 14.2, 1H, Npt CH$_2$), 1.06 (s, 9H, Npt CMe$_3$), 1.24 (s, 3H, allyl Me), 1.61 (m, 1H, allyl CH$_2$), 1.82 (s, 15H, C$_5$Me$_5$), 2.55 (m, 1H, allyl CH$_2$), 4.40 (m, 1H, allyl CH). ^{13}C{^{1}H} NMR (75 MHz, CD$_2$Cl$_2$) δ 10.2 (C$_5$*Me*$_5$), 19.5, 30.7 (allyl Me), 34.3 (Npt C*Me*$_3$), 37.6 (allyl CH$_2$), 39.9 (Npt *C*Me$_3$), 40.7 (Npt CH$_2$), 101.7 (allyl CH), 107.5 (*C*$_5$Me$_5$), 147.8 (allyl C). Sel NOE (400 MHz, C$_6$D$_6$) δ irrad. at 4.45, NOE at 1.02, irrad. at 0.67, NOE at 1.02, 1.42, 1.52, and 2.55. Anal. Calcd for C$_{20}$H$_{35}$NOW: C, 49.09; H, 7.21; N, 2.86. Found: C, 49.16; H, 7.03; N, 2.87.

Preparation of Cp*W(NO)(CH$_2$CMe$_3$)(η³-CH$_2$CMeCH$_2$) (2). Complex **2**was synthesized from the reaction between Cp*W(NO)(CH$_2$CMe$_3$)Cl (2.00 g, 4.40 mmol) and (CH$_2$-CMeCH$_2$)$_2$Mg·*x*(dioxane) (titer = 113.0 g/mol R, 0.501 g, 0.5 equiv). Complex **2** was worked up in a manner similar to that for **1** and was isolated as long pale-yellow needles (0.65 g, 62%).

2: IR (cm^{-1}) 1563 (s, ν_{NO}). ^{1}H NMR (400 MHz, C$_6$D$_6$) δ 0.56 (br d, $^2J_{HH}$ = 2.7, 1H, allyl CH$_2$), 1.06 (d, $^2J_{HH}$ = 13.0, 1H, C*H*$_2$CMe$_3$), 1.35 (s, 9H, CMe$_3$), 1.50 (s, 15H, C$_5$Me$_5$), 1.73 (d, $^2J_{HH}$ = 13.0, 1H, C*H*$_2$CMe$_3$), 1.79 (br s, 1H, allyl CH$_2$), 2.02 (dd, $^2J_{HH}$ = 2.7, $^4J_{HH}$ = 4.2, 1H, allyl CH$_2$), 2.28 (s, 3H, allyl Me), 3.52 (br d, $^4J_{HH}$ = 4.2, 1H, allyl CH$_2$). ^{13}C{^{1}H} NMR (100 MHz, C$_6$D$_6$) δ 9.9 (C$_5$*Me*$_5$), 21.8 (allyl Me), 27.4 (*C*H$_2$CMe$_3$), 35.0 (CH$_2$C*Me*$_3$) 37.4 (CH$_2$*C*Me$_3$), 43.5 (allyl CH$_2$), 74.5 (allyl CH$_2$), 106.5 (*C*$_5$Me$_5$), 129.5 (allyl *C*Me). MS (LREI, *m/z*, probe temperature 120 °C) 475 [M$^+$]. Anal. Calcd for C$_{19}$H$_{33}$NOW: C, 48.01; H, 7.00; N, 2.95. Found: C, 48.13; H, 7.12; N, 3.17.

Preparation of Cp*W(NO)(CH$_2$CMe$_3$)(η³-CH$_2$CHCHMe) (3). Complex **3** was synthesized from the reaction between Cp*W(NO)(CH$_2$CMe$_3$)Cl (3.20 g, 7.03 mmol) and (CH$_2$-CHCHMe)$_2$Mg·*x*(dioxane) (titer = 112.5 g/mol R, 0.791 g, 0.5 equiv). Since complex **3** is thermally unstable, cold solvents (−30 °C) had to be employed throughout its extraction and subsequent chromatography to minimize its decomposition. The residue from the chromatographic eluate was redissolved and crystallized from pentane at −30 °C overnight to obtain **3** as orange-yellow crystalline, irregularly shaped clusters in multiple crops. The solids were washed with small amounts of cold pentane (−30 °C, 2 × 5 mL) and then dried in vacuo. Yield 2.22 g (43%).

3: IR (cm^{-1}) 1594 (s, ν_{NO}). ^{1}H NMR (400 MHz, C$_6$D$_6$) δ (major isomer) 0.89 (d, $^2J_{HH}$ = 13.2, 1H, C*H*$_2$CMe$_3$), 1.01 (m, 1H, allyl C*H*Me), 1.32 (s, 9H, CMe$_3$), 1.48 (s, 15H, C$_5$Me$_5$), 1.56 (d, $^3J_{HH}$ = 14.0, 1H, allyl CH$_2$), 1.59 (d, $^2J_{HH}$ = 13.2, 1H, C*H*$_2$CMe$_3$), 1.89 (d, $^3J_{HH}$ = 6.0, 3H, allyl Me), 3.67 (d, $^3J_{HH}$ = 7.2 1H, allyl CH$_2$), 4.97 (ddd, $^3J_{HH}$ = 7.2, $^3J_{HH}$ = 9.4, $^3J_{HH}$ = 14.0, 1H, allyl CH). δ (minor isomer) selected signals 0.51 (m, 1H, allyl CH$_2$), 1.35 (s, 9H, CMe$_3$), 2.30 (m, 1H, allyl CH$_2$), 2.67 (m, 1H, allyl CH), 4.47 (m, 1H, allyl CH). ^{13}C{^{1}H} NMR (100 MHz, C$_6$D$_6$) δ 9.5 (C$_5$*Me*$_5$), 16.9 (allyl Me), 27.9 (*C*H$_2$CMe$_3$), 34.6 (CH$_2$C*Me*$_3$), 39.3 (CH$_2$*C*Me$_3$), 52.4 (allyl *C*HMe), 74.3 (allyl CH$_2$), 106.0 (*C*$_5$Me$_5$), 114.6 (allyl *C*H). MS (LREI, *m/z*, probe temperature 120 °C) 475 [M$^+$]. Anal. Calcd for C$_{19}$H$_{33}$NOW: C, 48.01; H, 7.00; N, 2.95. Found: C, 47.88; H, 7.32; N, 3.24.

Preparation of Cp*W(NO)(CH$_2$CMe$_3$)(η³-CH$_2$CHCHPh) (4). Complex **4** was synthesized from Cp*W(NO)(CH$_2$CMe$_3$)Cl (0.50 g, 1.10 mmol) and (CH$_2$CHCHPh)$_2$Mg·*x*(dioxane) (titer = 187.0 g/mol R, 0.205 g, 0.5 equiv) and worked up in a manner similar to that described for **1** above. The orange filtrate was collected, the solvent was removed in vacuo, and the residue was crystallized from pentane at −30 °C overnight to obtain **4** as orange rods. The crystals were washed with small amounts of cold pentane (−30 °C, 2 × 2 mL) and then dried in vacuo. Yield 0.34 g (58%).

4: IR (cm^{-1}) 1588 (s, ν_{NO}). ^{1}H NMR (400 MHz, C$_6$D$_6$) δ 0.93 (br s, 1H, C*H*$_2$CMe$_3$), 1.24 (obscured, 1H, allyl H), 1.32 (br s, 9H, CMe$_3$), 1.43 (br s, 15H, C$_5$Me$_5$), 1.60 (br s, 1H, C*H*$_2$CMe$_3$), 2.11 (br s, 1H, allyl H), 3.74 (br s, 1H, allyl H), 5.53 (br s, 1H, allyl CH), 7.07–7.36 (br m, 5H, aryl H). ^{13}C{^{1}H} NMR (100 MHz, C$_6$D$_6$) δ 9.5 (C$_5$*Me*$_5$), 29.1 (*C*H$_2$CMe$_3$), 34.8 (CH$_2$C*Me*$_3$), 39.0 (CH$_2$*C*Me$_3$), 61.1 (allyl *C*HPh), 72.0 (allyl CH$_2$), 106.3 (*C*$_5$Me$_5$), 109.1 (allyl *C*H), 126.4 (aryl C), 127.2 (aryl C), 128.7 (aryl C), 137.4 (ipso C). MS (LREI, *m/z*, probe temperature 120 °C) 537 [M$^+$]. Anal. Calcd for C$_{19}$H$_{33}$NOW: C, 53.64; H, 6.56; N, 2.61. Found: C, 53.58; H, 6.32; N, 2.64.

Preparation of Cp*W(NO)(CH$_2$SiMe$_3$)(η³-CH$_2$CHCHMe) (5). Complex **5** was synthesized from the reaction between Cp*W(NO)(CH$_2$SiMe$_3$)Cl (1.93 g, 4.40 mmol) and (CH$_2$-CHCHMe)$_2$Mg·*x*(dioxane) (titer = 112.5 g/mol R, 0.501 g, 0.5

equiv). Complex **5** was worked up in a manner identical with that described for **1**. Complex **5** was crystallized as yellow-orange prisms (1.10 g, 65%).

5: IR (cm^{-1}) 1593 (s, ν_{NO}). ^1H NMR (300 MHz, C_6D_6) (two isomers are present in an approximately 3:1 ratio): δ (major isomer) −0.62 (d, $^2J_{HH}$ = 13.2, 1H, CH_2SiMe$_3$), −0.09 (d, $^2J_{HH}$ = 13.2, 1H, CH_2SiMe$_3$), 0.37 (s, 9H, SiMe$_3$), 1.01 (m, 1H, allyl C*H*Me), 1.48 (s, 15H, C$_5$Me$_5$), 1.58 (d, $^3J_{HH}$ = 13.8, 1H, allyl CH$_2$), 1.88 (d, $^3J_{HH}$ = 5.8, 3H, allyl Me), 3.36 (d, $^3J_{HH}$ = 7.0 1H, allyl CH$_2$), 5.10 (ddd, $^3J_{HH}$ = 13.8, $^3J_{HH}$ = 9.4, $^3J_{HH}$ = 7.0, 1H, allyl CH). δ (minor isomer) selected signals −0.76 (d, $^2J_{HH}$ = 13.2, 1H, CH_2SiMe$_3$), −0.48 (d, $^2J_{HH}$ = 13.2, 1H, CH_2SiMe$_3$), 0.40 (s, 9H, SiMe$_3$), 1.34 (d, $^3J_{HH}$ = 5.8, 3H, allyl Me), 1.49 (s, 15H, C$_5$Me$_5$), 2.12 (m, 1H, allyl CH$_2$), 2.24 (m, 1H, allyl CH), 4.61 (m, 1H, allyl CH). $^{13}C\{^1H\}$ NMR (75 MHz, C_6D_6) δ −6.2 (*C*H$_2$SiMe$_3$), 4.1 (CH$_2$Si*Me*$_3$), 10.3 (C$_5$*Me*$_5$), 17.1 (allyl Me), 53.3 (allyl *C*HMe), 74.5 (allyl CH$_2$), 106.5 (*C*$_5$Me$_5$), 114.2 (allyl *C*H). MS (LREI, *m/z*, probe temperature 100 °C) 491 [M$^+$]. Anal. Calcd for $C_{18}H_{33}NOW$: C, 44.00; H, 6.77; N, 2.85. Found: C, 44.04; H, 6.90; N, 2.85.

Preparation of Cp*W(NO)(CH$_2$CMe$_3$)(η^3-C$_3$H$_5$) (6). Complex **6** was synthesized from Cp*W(NO)(CH$_2$CMe$_3$)Cl (2.50 g, 5.50 mmol) and (C$_3$H$_5$)$_2$Mg·*x*(dioxane) (titer = 98.0 g/mol R, 0.538 g, 0.5 equiv) and worked up in a manner similar to that described for **1** above. The final reaction mixture was taken to dryness in vacuo, and the residue was extracted with hexanes (4 × 100 mL). The combined extracts were transferred to the top of a neutral activated alumina(I) column (2 × 8 cm) made up in hexanes and supported on a medium porosity frit. The column was eluted with 1:1 hexanes/Et$_2$O, and the resulting yellow band was collected. Solvents were removed from the eluate in vacuo to obtain a yellow microcrystalline powder that was recrystallized from 3:1 pentane/Et$_2$O at −30 °C. Fluffy, bright-yellow needles of **6** were obtained in multiple crops. The crystals were washed with small amounts of cold pentane (−30 °C, 2 × 5 mL) and dried in vacuo. Yield 1.70 g (62%).

6: IR (cm^{-1}) 1597 (s, ν_{NO}). ^1H NMR (400 MHz, C_6D_6) δ 0.49 (br s, 1H, allyl CH$_2$), 0.92 (d, $^2J_{HH}$ = 12.4, 1H, CH_2CMe$_3$), 1.30 (s, 9H, CMe$_3$), 1.49 (s, 15H, C$_5$Me$_5$), 1.67 (d, $^2J_{HH}$ = 12.4, 1H, CH_2CMe$_3$), 1.89 (br s, 1H, allyl CH$_2$), 2.29 (br s, 1H, allyl CH$_2$), 3.78 (br s, 1H, allyl CH$_2$), 5.12 (m, allyl CH). $^{13}C\{^1H\}$ NMR (100 MHz, C_6D_6) δ 9.8 (C$_5$*Me*$_5$), 26.7 (*C*H$_2$CMe$_3$), 34.5 (CH$_2$C*Me*$_3$), 39.1 (CH$_2$*C*Me$_3$), 40.0 (allyl CH$_2$), 78.9 (allyl CH$_2$), 106.1 (*C*$_5$Me$_5$), 111.8 (allyl *C*Me). MS (LREI), *m/z*, probe temperature 120 °C) 461 [M$^+$]. Anal. Calcd for $C_{18}H_{31}NOW$: C, 46.87; H, 6.77; N, 3.03. Found: C, 46.95; H, 7.10; N, 3.07.

Preparation of Cp*W(NO)(CH$_2$CMe$_3$)(NC$_4$H$_7$-2-Me$_2$-CCH=CH$_2$) (7). Complex **7** was prepared by stirring a solution of **1** (97.1 mg, 0.199 mmol) in pyrrolidine (2 mL) for 17 h at room temperature. The final reaction mixture was taken to dryness in vacuo, and the residue was dissolved in a minimum of pentane. The pentane solution was chromatographed on a column of alumina (1 × 3 cm) with pentane as eluant to develop a single orange band that was eluted and collected. Concentration of the eluate under reduced pressure and cooling at −30 °C overnight resulted in the deposition of **7** as an orange crystalline solid (58.1 mg, 52% yield).

7: IR (cm^{-1}) 1561 (s, ν_{NO}). MS (LREI, *m/z*, probe temperature 120 °C) 558 [P$^+$, ^{184}W], 489 [P-allyl$^+$, ^{184}W]. ^1H NMR (500 MHz, C_6D_6) δ 0.67 (d, $^2J_{HH}$ = 14.09, 1H, CH_2CMe$_3$), 1.06 (s, 3H, Me$_2$C), 1.17 (s, 3H, Me$_2$C), 1.18 (d, $^2J_{HH}$ = 14.09, 1H, CH_2CMe$_3$), 1.36 (s, 9H, CMe$_3$), 1.48–1.61 (m, 3H, pyrrolidine H), 1.67 (s, 15H, C$_5$Me$_5$), 1.80–1.89 (m, 1H, pyrrolidine H), 3.00 (m, 1H, pyrrolidine NCH$_2$), 3.20 (m, 1H, pyrrolidine NCH$_2$), 4.89–5.00 (m, 3H, pyrrolidine NCH and *H*$_2$C=CH). 5.81 (dd, $^3J_{HH}$ = 17.5, $^3J_{HH}$ = 10, 1H, H$_2$C=C*H*). $^{13}C\{^1H\}$ NMR (125 MHz, C_6D_6) δ 10.0 (C$_5$*Me*$_5$), 23.6 (Me$_2$*C*), 23.8 (pyrrolidine CH$_2$), 24.0 (*Me*$_2$C), 24.5 (*Me*$_2$C), 28.0 (pyrrolidine CH$_2$), 34.4 (CH$_2$C*Me*$_3$), 37.1 (CH$_2$*C*Me$_3$), 54.4 (*C*H$_2$CMe$_3$), 58.9 (pyrrolidine NCH$_2$), 85.0 (pyrrolidine NCH), 110.2 (*C*$_5$Me$_5$), 111.8 (*C*H$_2$=CH), 146.4 (CH$_2$=*C*H). Anal. Calcd for $C_{24}H_{42}N_2OW$: C, 51.62; H, 7.58; N, 5.02. Found: C, 51.93; H, 7.90; N, 5.01.

Preparation of Cp*W(NO)(CH$_2$CMe$_3$)(NC$_5$H$_9$-2-Me$_2$CCH=CH$_2$) (8). Complex **8** was prepared by stirring a solution of **1** (90.3 mg, 0.185 mmol) in piperidine (2 mL) for 1 week at room temperature. The final reaction mixture was taken to dryness, and the residue was dissolved in a minimum amount of pentane. This solution was then chromatographed on a column of alumina (1 × 3 cm) with pentane as eluant to obtain an orange eluate that was collected. Concentration of the eluate under reduced pressure and cooling to −30 °C overnight resulted in the deposition of **8** as orange crystals (17 mg, 17%).

8: IR (cm^{-1}) 1564 (s, ν_{NO}). MS (LREI, *m/z*, probe temperature 120 °C) 572 [P$^+$, ^{184}W], 503 [P-allyl$^+$, ^{184}W]. ^1H NMR (500 MHz, C_6D_6) δ 1.10 (s, 3H, Me$_2$C), 1.20 (m, 1H, piperidine H), 1.23 (s, 3H, Me$_2$C), 1.29 (d, $^2J_{HH}$ = 5.92, 1H, CH_2CMe$_3$), 1.36 (m, 1H, piperidine H), 1.41 (s, 9H, CMe$_3$), 1.50 (m, 1H, piperidine H), 1.69 (d, $^2J_{HH}$ = 5.92, 1H, CH_2CMe$_3$), 1.69 (s, 15H, C$_5$Me$_5$), 1.72–1.75 (m, 2H, piperidine H), 2.03–2.05 (m, 1H, piperidine H), 3.01 (br d, 1H, piperidine NCH$_2$), 3.63 (td, $^3J_{HH}$ = 12, $^4J_{HH}$ = 3.2, 1H, piperidine NCH$_2$), 4.91 (d, $^3J_{HH}$ = 10.7, 1H, *H*$_2$C=CH), 4.96 (d, $^3J_{HH}$ = 17.4, 1H, *H*$_2$C=CH) 5.09–5.11 (br,1H, piperidine NCH), 6.05 (dd, $^3J_{HH}$ = 17.46, $^3J_{HH}$ = 10.7, 1H, CH$_2$=C*H*). $^{13}C\{^1H\}$ NMR (125 MHz, C_6D_6) δ 10.0 (C$_5$*Me*$_5$), 20.4 (piperidine CH$_2$), 23.5 (*Me*$_2$C), 26.4 (piperidine CH$_2$), 26.6 (*Me*$_2$C), 27.6 (piperidine CH$_2$), 34.6 (CH$_2$C*Me*$_3$), 37.0 (CH$_2$*C*Me$_3$), 49.4 (*C*H$_2$CMe$_3$), 56.0 (piperidine NCH$_2$), 81.4 (piperidine NCH), 110.3 (*C*$_5$Me$_5$), 110.8 (*C*H$_2$=CH), 148.9 (CH$_2$=*C*H). The signal for CH$_2$=CH−*C*Me$_2$ is probably obscured. Anal. Calcd for $C_{25}H_{44}N_2OW$: C, 52.45; H, 7.75; N, 4.89. Found: C, 52.18; H, 7.74; N, 5.29.

Preparation of Cp*W(NO)(CH$_2$CMe$_3$)(NC$_4$H$_7$-2-CH$_2$CMe=CH$_2$) (9). In a small Schlenk tube complex **2** (95.0 mg, 0.200 mmol) was dissolved in pyrrolidine (2 mL), and the mixture was stirred under a gentle flow of N_2 for 64 h, after which time the volatiles were removed in vacuo. The orange-yellow residue was redissolved in a minimum of pentane and chromatographed on alumina, using 3:1 pentane/Et$_2$O as eluant. The orange band that developed was eluted from the column and collected, and the solvent was removed in vacuo from the eluate. NMR spectroscopy revealed that the residue was an approximately 60:40 mixture of **2** (starting material) and **9**. The yellow-orange solid was extracted with cold pentane (−30 °C, 2 × 3 mL), leaving behind mostly **2**, which was the less soluble of the two species. The extracts were combined and reduced in volume. Complex **9** was fractionally crystallized as fine yellow-orange rods (18 mg, 16%). Longer reaction times led to the decomposition of **9** into an off-white solid.

9: IR (cm^{-1}) 1563 (s, ν_{NO}). ^1H NMR (400 MHz, C_6D_6) δ 0.79 (d, $^2J_{HH}$ = 14.0, 1H, CH_2CMe$_3$), 0.97 (d, $^2J_{HH}$ = 14.0, 1H, CH_2CMe$_3$), 1.39 (s, 9H, CH$_2$C*Me*$_3$), 1.47 (m, 1H, pyrrolidine CH$_2$), 1.65 (s, 15H, C$_5$Me$_5$), 1.70 (m, 1H, pyrrolidine CH$_2$), 1.95 (t, $^3J_{HH}$ = 11.6, 1H, H$_2$C=CMe−C*H*$_2$), 1.96 (s, 3H, H$_2$C=C*Me*), 2.74 (dd, $^3J_{HH}$ = 4.0, $^3J_{HH}$ = 11.6, 1H, H$_2$C=CMe−C*H*$_2$), 3.03 (m, 2H, pyrrolidine NCH$_2$), 4.80–4.83 (overlapping br s, 2H, *H*$_2$C=CMe), 5.14 (m, 1H, pyrrolidine NCH). Other pyrrolidine CH$_2$ signals are obscured. $^{13}C\{^1H\}$ NMR (100 MHz, C_6D_6) δ 9.6 (C$_5$*Me*$_5$), 22.2 (H$_2$C=C*Me*), 26.0 (pyrrolidine CH$_2$), 31.0 (pyrrolidine CH$_2$), 34.6 (CH$_2$C*Me*$_3$), 37.3 (CH$_2$*C*Me$_3$), 50.1 (H$_2$C=CMe−*C*H$_2$), 57.9 (pyrrolidine N*C*H$_2$), 58.4 (*C*H$_2$CMe$_3$), 75.0 (pyrrolidine NCH), 109.7 (*C*$_5$Me$_5$), 112.2 (H$_2$*C*=CMe), 144.5 (H$_2$C=*C*Me). MS (LREI, *m/z*, probe temperature 120 °C) 544 [M$^+$], 489 [M − allyl$^+$]. Anal. Calcd for $C_{23}H_{40}N_2OW$: C, 50.74; H, 7.41; N, 5.15. Found: C, 50.63; H, 7.38; N, 5.03.

The reaction was also performed in a sealed vessel to detect the H_2 being evolved. A 250-mL bomb was charged with complex **2** (ca. 35.0 mg) and a small stir bar. Pyrrolidine (ca. 5 mL) was added via vacuum transfer, and the contents were stirred for 1 d. The volatiles, including an appropriate amount of pyrrolidine (ap-

proximately 0.75 mL), were then vacuum-transferred into a J. Young NMR tube equipped with a C_6D_6 capillary. The presence of H_2 was indicated by a singlet at 4.80 ppm in the ^{1}H NMR spectrum. This chemical shift was confirmed by recording the ^{1}H NMR spectrum of a separately prepared sample of H_2 in pyrrolidine in a J. Young NMR tube equipped with a C_6D_6 capillary.

Preparation of Cp*W(NO)(CH_2CMe_3)(NC_4H_7-2-CHMeCH=CH_2) (10). Complex **10** was synthesized in a manner similar to that described above for the preparation of complex **7**. The ^{1}H NMR spectrum of the final product mixture in C_6D_6 indicated the formation of at least two new organometallic species, with compound **10** being the major product. The orange-brown crude product residue was redissolved in a minimum of pentane, and the solution was chromatographed on alumina with 3:1 pentane/Et_2O as eluant. The orange band that developed was eluted from the column and collected. Solvent was removed from the eluate in vacuo, resulting in the recovery of **10**. The minor products appeared to have decomposed on the column. Complex **10** was recrystallized from pentane at −30 °C overnight to obtain an orange-yellow microcrystalline solid (18 mg, 22%).

10: IR (cm^{-1}) 1563 (s, ν_{NO}). ^{1}H NMR (400 MHz, C_6D_6) δ 0.72 (d, $^2J_{HH}$ = 14.4, 1H, CH_2CMe$_3$), 0.88 (d, $^3J_{HH}$ = 6.8, 3H, H$_2$C=CH−CH*Me*), 1.10 (d, $^2J_{HH}$ = 14.4, 1H, CH_2CMe$_3$), 1.35 (obscured, 2H, pyrrolidine CH_2), 1.37 (s, 9H, CMe_3), 1.48 (m, 1H, pyrrolidine CH_2), 1.67 (s, 15H, C_5Me_5), 1.70 (obscured, 1H, pyrrolidine CH_2), 2.79 (m, 1H, H$_2$C=CH−C*H*Me), 3.02 (m, 2H, pyrrolidine NCH_2), 5.01–5.03 (m, 2H, pyrrolidine NCH and H_2C=CH), 5.16 (d, $^3J_{HH}$ = 17.2, 1H, H_2C=CH), 5.99 (ddd, $^3J_{HH}$ = 7.2, $^3J_{HH}$ = 10.4, $^3J_{HH}$ = 17.2,1H, H$_2$C=C*H*). ^{13}C{^{1}H} NMR (100 MHz, C_6D_6) δ 9.8 (C_5Me_5), 14.6 (H$_2$C=CH−CH*Me*), 25.5 (pyrrolidine CH_2), 28.7 (pyrrolidine CH_2), 34.5 (CH$_2$C*Me*$_3$), 37.1 (CH$_2$*C*Me$_3$), 45.6 (H$_2$C=CH−*C*HMe), 55.1 (*C*H$_2$CMe$_3$), 58.6 (pyrrolidine NCH_2), 80.6 (pyrrolidine NCH), 109.9 (C_5Me$_5$), 114.1 (H$_2$*C*=CH), 142.9 (H$_2$C=*C*H). MS (LREI, *m*/*z*, probe temperature 120 °C) 544 [M$^+$], 489 [M − allyl$^+$]. Anal. Calcd for $C_{23}H_{40}N_2OW$: C, 50.74; H, 7.41; N, 5.15. Found: C, 51.03; H, 7.50; N, 4.94.

Preparation of Cp*W(NO)(CH_2CMe_3)(NC_4H_7-2-CHPhCH=CH_2) (11). Complex **11** was synthesized from **4** (30 mg, 0.558 mmol) and pyrrolidine (2 mL) in a manner identical with that described above for the preparation of complex **7**. The ^{1}H NMR spectrum of the crude product in C_6D_6 revealed the quantitative conversion of **4** into **11**. Complex **11** was worked up in a manner identical with that described above for complex **7**. Complex **11** was crystallized from pentane at −30 °C overnight to obtain an orange-yellow microcrystalline solid (24 mg, 71%).

11: IR (cm^{-1}) 1562 (s, ν_{NO}). ^{1}H NMR (400 MHz, C_6D_6) δ 0.86 (d, $^2J_{HH}$ = 14.0, 1H, CH_2CMe$_3$), 1.07 (d, $^2J_{HH}$ = 14.0, 1H, CH_2CMe$_3$), 1.39 (s, 9H, CMe_3), 1.71 (s, 15H, C_5Me_5), 3.00–3.15 (m, 3H, PhC*H* and pyrrolidine NCH_2), 4.89 (dd, $^2J_{HH}$ = 1.4, $^3J_{HH}$ = 16.9, 1H, H_2C=CH), 5.02 (dd, $^2J_{HH}$ = 1.4, $^3J_{HH}$ = 10.0, 1H, H_2C=CH), 5.59 (m, 1H, pyrrolidine NCH), 6.78 (dt, $^3J_{HH}$ = 10.0, $^3J_{HH}$ = 16.9,1H, H$_2$C=C*H*), 7.01 (m, 1H para CH), 7.11 (m, 2H, meta CH), 7.32 (m, 2H, ortho CH). Other pyrrolidine CH_2 signals are obscured. ^{13}C{^{1}H} NMR (100 MHz, C_6D_6) δ 10.0 (C_5Me_5), 23.3 (pyrrolidine CH_2), 29.2 (pyrrolidine CH_2), 34.5 (CH$_2$C*Me*$_3$), 37.0 (CH$_2$*C*Me$_3$), 53.2 (*C*H$_2$CMe$_3$), 55.8 (pyrrolidine NCH_2), 56.1 (*C*HPh), 82.8 (pyrrolidine NCH), 110.3 (C_5Me$_5$), 115.2 (H$_2$*C*=CH), 126.6 (Ar C), 128.5 (Ar C), 129.1 (Ar C), 143.0 (H$_2$C=*C*H), 144.3 (Ar ipso C). MS (LREI, *m*/*z*, probe temperature 120 °C) 606 [M$^+$]. Anal. Calcd for $C_{28}H_{42}N_2OW$: C, 55.44; H, 6.98; N, 4.62. Found: C, 55.23; H, 7.20; N, 4.77.

Preparation of Cp*W(NO)(CH_2SiMe_3)(NC_4H_7-2-CHMeCH=CH_2) (12). Complex **12** was synthesized by dissolving **5** (30 mg, 0.56 mmol) in pyrrolidine (2 mL) for 4 d. The ^{1}H NMR spectrum of the crude product in C_6D_6 revealed the quantitative conversion of **5** into **12**. Unfortunately, multiple attempts to obtain **12** as a tractable solid were unsuccessful.

12: IR (cm^{-1}) 1561 (s, ν_{NO}). ^{1}H NMR (400 MHz, C_6D_6) δ −0.50 (overlapping d, 2H, CH_2SiMe$_3$), 0.38 (s, 9H, CMe_3), 1.67 (s, 15H, C_5Me_5), 2.90–3.08 (m, 3H, MeC*H* and pyrrolidine NCH_2), 4.97–5.03 (m, 2H, pyrrolidine NCH and H_2C=CH), 5.17 (d, $^3J_{HH}$ = 17.2, 1H, H_2C=CH), 5.98 (ddd, $^3J_{HH}$ = 7.2, $^3J_{HH}$ = 10.4, $^3J_{HH}$ = 17.2, 1H, H$_2$C=C*H*). Other pyrrolidine CH_2 signals are obscured. ^{13}C{^{1}H} NMR (100 MHz, C_6D_6) δ −7.0 (*C*H$_2$SiMe$_3$), 3.3 (CH$_2$Si*Me*$_3$), 9.9 (C_5Me_5), 14.5 (H$_2$C=CH−CH*Me*), 25.8 (pyrrolidine CH_2), 27.5 (pyrrolidine CH_2), 45.3 (H$_2$C=CH−*C*HMe), 58.6 (pyrrolidine NCH_2), 80.9 (pyrrolidine NCH), 109.0 (C_5Me$_5$), 114.1 (H$_2$*C*=CH), 142.8 (H$_2$C=*C*H). MS (LREI, *m*/*z*, probe temperature 120 °C) 560 [M$^+$].

Preparation of Cp*W(NO)(NC_4H_8)(CHMeCH$_2$$NC_4H_8$) (13). In a 4-dram vial inside a glovebox complex **2** (46 mg, 0.10 mmol) was dissolved in excess pyrrolidine (2 mL). The mixture was allowed to stand for 5 h, after which time the pyrrolidine was removed in vacuo. The orange-brown residue was redissolved in pentane, and the solution was filtered through Celite. Subsequent concentration of the filtrate and cooling to −30 °C overnight afforded **13** as thin orange needles (21 mg, 40%). X-ray quality crystals of **13** were obtained when Et_2O was employed as the crystallization solvent.

13: IR 1553 (s, ν_{NO}). ^{1}H NMR (400 MHz, C_6D_6) (selected signals) δ 1.18–1.46 (m, 5H, pyrrolidyl CH_2), 1.54 (d, $^3J_{HH}$ = 7.2, 3H, WCHMe), 1.72 (s, 15H, C_5Me_5 and m, 1H, WC*H*Me), 2.51 (m, 2H, CNCH$_2$), 2.76 (m, 2H, CNCH$_2$), 2.83 (m, 1H, WNCH$_2$), 3.11 (m, 1H, WNCH$_2$), 3.43 (dd, $^2J_{HH}$ = 12.0, $^3J_{HH}$ = 3.9, 1H, WCHMeC*H*$_2$), 3.60 (t, $^2J_{HH}$ = 12.0, $^3J_{HH}$ = 12.0, WCHMeC*H*$_2$), 4.03 (m, 1H, WNCH$_2$), 4.34 (m, 1H, WNCH$_2$). ^{13}C{^{1}H} NMR (100 MHz, C_6D_6) δ 9.5 (C_5Me_5), 21.1 (WCH*Me*), 24.1, 26.3, 26.5 (pyrrolidyl CH_2), 42.9 (W*C*HMe), 53.8 (pyrrolidyl CN*C*H$_2$), 58.0, 67.5 (WN*C*H$_2$), 68.2 (WCHMe*C*H$_2$), 109.9 (C_5Me$_5$). MS (LREI, *m*/*z*, probe temperature 100 °C) 531 [M$^+$]. Anal. Calcd for $C_{21}H_{37}N_3OW$: C, 47.47; H, 7.02; N, 7.91. Found: C, 47.34; H, 6.96; N, 7.85.

Preparation of Cp*W(NO)(NC_5H_{10})(CHMeCH$_2$$NC_5H_{10}$) (14). In a 4-dram vial inside a glovebox complex **2** (92 mg, 0.200 mmol) was dissolved in excess piperidine (2 mL). The mixture was allowed to stand for 2 d, after which time the piperidine was removed in vacuo. The orange-brown residue was extracted with pentane, leaving behind an off-white unidentifiable residue. The extracts were filtered through Celite. Subsequent concentration and cooling of the filtrate to −30 °C overnight afforded **14** as orange needles (22 mg, 21%).

14: IR 1561 (s, ν_{NO}). ^{1}H NMR (400 MHz, C_6D_6) (selected signals) δ 1.20–1.50 (m, pyrrolidyl CH_2), 1.64 (d, $^3J_{HH}$ = 7.2, 3H, WCHMe), 1.71 (s, 15H, C_5Me_5), 2.39 (m, 2H, CNCH$_2$), 2.77 (m, 2H, CNCH$_2$), 3.05 (m, 1H, WNCH$_2$), 3.17 (m, 1H, WNCH$_2$), 3.38 (t, $^2J_{HH}$ = 12.0, $^3J_{HH}$ = 12.0, WCHMeC*H*$_2$), 3.54 (dd, $^2J_{HH}$ = 12.0, $^3J_{HH}$ = 3.9, 1H, WCHMeC*H*$_2$), 3.90 (m, 1H, WNCH$_2$), 4.64 (m, 1H, WNCH$_2$). ^{13}C{^{1}H} NMR (100 MHz, C_6D_6) δ 9.6 (C_5Me_5), 21.1 (WCH*Me*), 24.3, 25.6, 26.9, 28.2, 29.0 (piperidyl CH_2), 41.3 (W*C*HMe), 54.8 (pyrrolidyl CN*C*H$_2$), 60.7, 70.3 (WN*C*H$_2$), 71.7 (WCHMe*C*H$_2$), 109.9 (C_5Me$_5$). MS (LREI, *m*/*z*, probe temperature 100 °C) 559 [M$^+$]. Anal. Calc. for $C_{23}H_{41}NOW$: C, 49.36; H, 7.39; N, 7.51. Found: C, 49.24; H, 7.26; N, 7.47.

X-ray Crystallography. Data collection for each compound was carried out at −100 ± 1 °C on a Rigaku AFC7/ADSC CCD diffractometer or on a Bruker X8 APEX diffractometer, using graphite-monochromated Mo Kα radiation.

Data for **3** were collected to a maximum 2θ value of 55.8° in 0.5° oscillations. The structure was solved by direct methods[21] and

(21) SIR92 Altomare, A.; Cascarano, M.; Giacovazzo, C.; Guagliardi, A *J. Appl. Crystallogr.* **1993**, *26*, 343.

expanded by using Fourier techniques.[22] All non-hydrogen atoms were refined anisotropically; hydrogen atoms H1a, H1b, H2, H3, H5a, and H5b were refined isotropically, and all other hydrogen atoms were included in fixed positions. The final cycle of full-matrix least-squares analysis was based on 4599 observed reflections and 232 variable parameters.

Data for **4** were collected to a maximum 2θ value of 55.8° in 0.5° oscillations. The structure was solved by direct methods[21] and expanded by using Fourier techniques.[22] All non-hydrogen atoms were refined anisotropically; hydrogen atoms H1a, H1b, H2, and H3 were refined isotropically, and all other hydrogen atoms were included in fixed positions. The final cycle of full-matrix least-squares analysis was based on 5262 observed reflections and 268 variable parameters.

Data for **5** were collected to a maximum 2θ value of 60.8° in 0.5° oscillations. The structure was solved by direct methods[21] and expanded by using Fourier techniques.[22] The two isomers cocrystallized such that W1, C5, Si1, and the Cp* ligand were crystallographically equivalent in both compounds. The rest of the solution was modeled as two disordered parts, Part A (major isomer) and Part B (minor isomer), present in a 0.67 to 0.33 ratio. All non-hydrogen atoms were refined anisotropically, except for N1b, C6b, and C3b which were refined isotropically. All hydrogen atoms were included in fixed positions. The final cycle of full-matrix least-squares analysis was based on 5957 observed reflections and 278 variable parameters.

Data for **6** were collected to a maximum 2θ value of 56.1° in 0.5° oscillations. The structure was solved by direct methods[21] by using nonoverlapped data from the major twin component. Subsequent refinements were carried out by using an HKLF 5 format data set containing complete data from the major twin component and overlapped reflections of the second, minor component. All non-hydrogen atoms were refined anisotropically. All allyl hydrogens were located in difference maps and refined isotropically. All other hydrogen atoms were included in calculated positions but not refined. The batch scale refinement showed a roughly 82:18 ratio between the major and minor twin components. The final cycle of full-matrix least-squares refinement on F^2 was based on 31125 reflections from both twin components and 219 variable parameters.

Data for **7** were collected to a maximum 2θ value of 55.6° in 0.5° oscillations. The structure was solved by direct methods[21] and expanded by using Fourier techniques.[22] All non-hydrogen atoms were refined anisotropically. All hydrogen atoms were included in fixed positions. The final cycle of full-matrix least-squares analysis was based on 12520 observed reflections and 264 variable parameters.

Data for **8** were collected to a maximum 2θ value of 55.6° in 0.5° oscillations. The structure was solved by direct methods[21] and expanded by using Fourier techniques.[22] All non-hydrogen atoms were refined anisotropically. All hydrogen atoms were included in fixed positions. The final cycle of full-matrix least-squares analysis was based on 6277 observed reflections and 272 variable parameters.

Data for **9** were collected to a maximum 2θ value of 55.6° in 0.5° oscillations. The structure was solved by direct methods[21] and expanded by using Fourier techniques.[22] All non-hydrogen atoms were refined anisotropically. All hydrogen atoms were included in fixed positions. The final cycle of full-matrix least-squares analysis was based on 5392 observed reflections and 248 variable parameters.

Data for **13** were collected to a maximum 2θ value of 47.0° in 0.5° oscillations. The structure was solved by direct methods[21] and expanded by using Fourier techniques.[22] The crystal was twinned, and the crystallographic solution contained two molecules of **13**. In the second molecule, atom C10A was disordered in two positions in a 0.65 to 0.35 ratio and was modeled isotropically. All other non-hydrogen atoms were refined anisotropically, and all hydrogen atoms were included in fixed positions. The final cycle of full-matrix least-squares analysis was based on 11672 observed reflections and 481 variable parameters.

For each structure neutral-atom scattering factors were taken from Cromer and Waber.[23] Anomalous dispersion effects were included in F_{calc};[24] the values for $\Delta f'$ and $\Delta f''$ were those of Creagh and McAuley.[25] The values for mass attenuation coefficients are those of Creagh and Hubbell.[26] All calculations were performed with SHELXL-97.[27] X-ray crystallographic data for all eight structures are presented in Table 1, and full details of all crystallographic analyses are provided in the Supporting Information.

Acknowledgment. We are grateful to the Natural Sciences and Engineering Research Council of Canada for support of this work in the form of grants to P.L. We also thank Professor Jim Mayer for bringing the work in reference 4 to our attention and a reviewer for helpful comments.

Supporting Information Available: CIF files providing full details of crystallographic analyses of complexes **3**, **4**, **5**, **6**, **7**, **8**, **9**, and **13**. This material is available free of charge via the Internet at http://pubs.acs.org.

OM701236K

(22) Beurskens, P. T.; Admiraal, G.; Beurskens, G.; Bosman, W. P.; Garcia-Granda, S.; Gould, R. O.; Smits, J. M. M.; Smykalla, C. *PATTY*; University of Nijmegen, The Netherlands, 1992.

(23) Cromer, D. T.; Waber, J. T. *International Tables for X-ray Crystallography*; Kynoch Press: Birmingham, UK, 1974; Vol. IV.

(24) Ibers, J. A.; Hamilton, W. C. *Acta Crystallogr.* **1964**, *17*, 781–782.

(25) Creagh, D. C.; McAuley, W. J. *International Tables of X-ray Crystallography*; Kluwer Academic Publishers: Boston, MA, 1992; Vol. C.

(26) Creagh, D. C.; Hubbell, J. H. *International Tables for X-ray Crystallography*; Kluwer Academic Publishers: Boston, MA, 1992; Vol. C.

(27) Sheldrick, G. M. *SHELXL97*; University of Göttingen, Germany, 1997.